Dynamics of dislocations and surface instabilities in misfitting heteroepitaxial films

Mikko Haataja[1], Judith Müller[2], A. D. Rutenberg[3], and Martin Grant[1]

[1]*Centre for the Physics of Materials, Department of Physics, McGill University, Rutherford Building, 3600 rue University,*
Montréal, Québec H3A 2T8, Canada
[2]*Instituut-Lorentz for Theoretical Physics, University of Leiden, P.O. Box 9506, NL-2300 RA Leiden, The Netherlands*
[3]*Department of Physics, Dalhousie University, Halifax, Nova Scotia B3H 3J5, Canada*

We introduce a continuum model of elasticity in a nonequilibrium multiphase system — including smooth and singular strains, as well as their coupling to free surfaces — and apply it to the dynamics of misfitting heteroepitaxial films. Above a critical thickness, defects relieve strain, competing with an instability at the interface. Depending on their mobility, defects can screen stress by building up at large-curvature groove tips, leading to high ductility, or be "outrun" by the tips, leading to brittleness. Hence we find a nonequilibrium brittle to ductile transition.

PACS numbers: 62.20.Fe, 64.60.My, 68.55.-a

The properties of thin films can be tuned by growing them on a substrate which induces strain. However, such misfitting heteroepitaxial thin films can only be grown to a critical thickness. At that point, strain relaxes from the film as it either becomes plastic, or "buckles", and complex structure forms. Interest in this dynamical process goes back to the classic work of Frank and van der Merwe [1]. If one considers small strains where buckling is unimportant, Matthews and Blakeslee [2] derived the critical thickness at which coherency is lost through the appearance of misfit dislocations, which accommodate the applied strain. Alternatively, for large strains relief can occur without plasticity as the free surface becomes corrugated ("buckles") coherently, as identified in the stability analyses of Asaro and Tiller, [3] and of Grinfeld [4]. This latter mechanism is associated with dislocation-free Stranski-Krastanow growth in subcritical films [5–11].

In general both mechanisms are present. Misfit dislocations partially accommodate strain, and buckling occurs due to the residual strain. For example, controlled annealing experiments of Ozkan *et al.* [12] on supercritical SiGe films have demonstrated that groove alignment from the buckling depends on the presence of misfit dislocations. It is theoretically challenging to address both plasticity and buckling in this nonequilibrium process; the former involves singular contributions to the strain, while the latter constitutes a free boundary value problem. A molecular dynamics study of Dong *et al.* [13] addressed both aspects of the process and found a qualitative coupling between buckling and dislocation nucleation: the relaxation of misfit strain by dislocations occurred inside grooves, which came about by the relaxation of strain by buckling. Schwarz [14] studied misfit dislocation lines in three-dimensional static films in a quasi-equilibrium framework. Unfortunately, neither approach is viable for a quantitative study of the dynamics: molecular dynamics considers too short a time-scale, and the quasi-equilibrium approximation cannot explore how film geometry and dislocations evolve together. An alternate and appealing method is continuum mechanics, where the quantities entering constitutive relations, such as shear and bulk moduli, μ and κ, are straightforward to determine experimentally. Another benefit of such a coarse-grained approach is that the time evolution is on experimentally relevant scales.

In this Letter, we introduce a continuum model of elasticity in a nonequilibrium multiphase system, including smooth *and* singular strains, as well as their coupling to free surfaces. To show the usefulness of this approach, we have studied thin film morphology from the initial stages of instability of supercritical films to the fully nonlinear late-time regime. We find that the initial instability persists even with dislocations, with a growth rate that depends on the defect core energy and mobility. In the late-time regime, an island morphology forms with deep grooves if the defects cannot accommodate all strain — this is similar to that seen for subcritical films [7,9,10]. In contrast to the case of coherent buckling of thin films, we find that the dynamics of grooves are like those of crack tips in metals. Dislocations build up ahead of the groove tip, slowing it by screening some of the local stress. Furthermore, depending on the mobility of the dislocations, the film is either ductile (where the mobility is high enough that the defects keep pace with the growing groove tip) or brittle (where the groove tip outruns the dislocations). We find evidence for a dynamic brittle to ductile transition in groove dynamics, analogous to what occurs for cracks in fracture mechanics [15].

Following previous work by Onuki and Nishimore [16], and two of us [9], we introduce a Ginzburg-Landau free energy functional in terms of the local phase and elastic interactions. The order parameter $\phi(\vec{r},t)$, as a function of space $\vec{r}$ and time t, determines the equilibrium phase: vapor ($\phi_{eq} = 0$), film ($\phi_{eq} = 1$), or substrate ($\phi_{eq} = 2$). Elasticity involves the singular and nonsingular parts of the strain tensor $\mathbf{u}$, or, equivalently for the singular part,

the dislocation's Burger's vector $\vec{b}$. The free energy is

$$\mathcal{F} = \int_{\vec{r}} \left(\frac{\epsilon^2}{2} |\nabla\phi|^2 + f(\phi) + f_{\text{elastic}}(\phi, \mathbf{u}) \right), \qquad (1)$$

where the first term gives rise to a surface energy and well defined interfaces on the length scale of ϵ. The three phases are described by $f(\phi) = a\phi^4(\phi-1)^2(\phi-2)^2 + \frac{\eta^2}{2\kappa}\Phi_{\text{misfit}}^2$, where a controls the surface free energies. The externally applied misfit stress is proportional to [9] η, and Φ_{misfit} and Φ_{solid} are simple functions of ϕ [17] required to ensure that misfit stresses exist only in the film and that the shear modulus $\mu\Phi_{\text{solid}}$ vanishes in the vapor phase. For simplicity, we choose identical elastic moduli for the two solid phases.

The elastic part of the free energy has several parts: $f_{\text{elastic}} = f_{\text{smooth}} + f_{\text{sing}} + f_{\text{core}}$. The smooth part of the elastic energy [18,19] is defined in terms of the elastic moduli and the smooth strain fields u_{ij}, $f_{\text{smooth}} = \eta\Phi_{\text{misfit}}u_{kk} + \frac{1}{2}\kappa(u_{kk})^2 + \mu\Phi_{\text{solid}}(u_{ij} - \frac{\delta_{ij}}{2}u_{kk})^2$, where a summation convention is implicit over repeated indices. The singular part of the elastic energy is $f_{\text{sing}} = \frac{1}{2}\kappa(u_{kk}^s)^2 + \mu\Phi_{\text{solid}}(u_{ij}^s - \frac{\delta_{ij}}{2}u_{kk}^s)^2 + u_{ij}\sigma_{ij}^s$, where the last term gives the coupling between smooth strain and singular stress σ_{ij}^s defined below in terms of the Burger's vector $\vec{b}$. Depending on signs, the singular strain u_{ij}^s is able to match and relieve the smooth strain.

Since time scales of interest are much longer than elastic relaxation times, we employ the local mechanical equilibrium conditions $\nabla_j\sigma_{ij} = 0$. This permits us to integrate out the $\mathbf{u}$ to first order in μ/κ [9,16], giving rise to long-range elastic forces and the interactions between the dislocation cores. This gives $\sigma_{ij}^s = \epsilon_{ik}\epsilon_{jl}\nabla_k\nabla_l\chi$, where ϵ_{ij} denotes the antisymmetric unit tensor with $\epsilon_{xy} = 1$, and χ is the Airy stress function [18,19], that gives rise to the Peach-Koehler force between dislocations [20]. We restrict ourselves to two dimensions where χ is a scalar [21] determined by a biharmonic equation in the different phases [22,23]. Finally, the core energy of the defects is given by the sixth-order polynomial $f_{\text{core}} = \frac{1}{2}E_c|\vec{b}|^2 + c|\vec{b}|^2(b_0^2 - |\vec{b}|^2)^2$, where we will call E_c the energy of a dislocation, c is a constant, and the dislocation strength is b_0.

The dynamics of ϕ and $\vec{b}$ are driven by minimization of $\mathcal{F}$. For the order parameter

$$\tau\frac{\partial\phi}{\partial t} = -\frac{\delta\mathcal{F}}{\delta\phi} = \epsilon^2\nabla^2\phi - f'(\phi) - \frac{\chi}{4}\Phi_{\text{solid}}'\epsilon_{ij}\nabla_i b_j$$
$$- \frac{16\mu\eta^2}{\kappa^2}\left[2\Phi_{\text{misfit}}'m(\vec{r}) + \Phi_{\text{solid}}'n(\vec{r})\right] - \frac{\Phi_{\text{solid}}'\chi^2}{2Y\ell^4}$$
$$- \beta(\vec{r})\left[\frac{Y}{4}\Phi_{\text{solid}}'\epsilon_{ij}\nabla_i b_j - \frac{\Phi_{\text{solid}}'\chi}{\ell^4}\right] \qquad (2)$$

where primes on functions denote derivatives with respect to ϕ, τ^{-1} is a mobility, $Y = 4\kappa\mu/(\kappa+\mu)$ is Young's modulus, ℓ is a microscopic length [23], and long-range

elastic forces enter through [24] $m(\vec{r})$ and $n(\vec{r})$. The coupling $\beta(\vec{r}) \equiv \epsilon_{ij}\delta F/\delta(\nabla_i b_j)$ between the dislocations and σ_{ij} results from integrating the strain out of the dynamics [22,23]. For the dislocation densities

$$\frac{\partial b_i}{\partial t} = \left(m_g\nabla_x^2 + m_c\nabla_y^2\right)\frac{\delta\mathcal{F}}{\delta b_i} \qquad (3)$$
$$= \left(m_g\nabla_x^2 + m_c\nabla_y^2\right)\left[\frac{df_{\text{core}}}{db_i} + \frac{\epsilon_{ij}}{4}\nabla_j\left((\chi + Y\beta)\Phi_{\text{solid}}\right)\right],$$

where m_g and m_c denote the glide and climb mobilities. It proves sufficient to equilibrate the fields χ and β with a mixed real space–spectral method [23] every 10-30 Δt time steps, and in addition, to relax them dynamically after each time step with 50 Euler iterations. The phase field ϕ and dislocation densities $\vec{b}$ are updated using finite differencing on a scale of Δx for the spatial gradients and the Euler method for time evolution. System sizes considered were 128×128, 256×256, and 64×512. For the results reported $(\Delta x, \Delta t, \epsilon, \kappa, \ell, \tau, m_g) = (1, \leq 0.01, 1, 1, 2, 1, m_c)$. The climb mobility m_c was varied between 0.01 and 0.2, the core energy was controlled by varying E_c between 1 and 50, and dislocation densities were initialized with small random fluctuations of magnitude 10^{-4}. We report results for the supercritical regime where nucleation of defects does not control evolution. The remaining parameters $\vec{P} \equiv (a, \eta, \mu, c, b_0)$ are reported in context below.

With our approach, the physics of the film under external stress is clear. The smooth strain fields adjust to the stress by buckling, while the singular part of the internal strain adjusts to the stress by nucleating dislocations, if the core energy of those defects is not too large. Whether or not the dislocations can move fast enough to track the accumulation of local stress at the moving boundary is dependent upon their mobilities. For very early times, linear stability analysis describes the evolution. Our results, with and without defects, are summarized in Fig. 1 where we show the amplitude of the initial growth rate, for increasing core energies $E_c = 1$, 50, and ∞, $m_c = 0.01$, and in the inset interface profiles at $t \leq 25$. We initialized the system with a sinusoidal interface deformation of small amplitude h_0 and wave number q, with parameters $\vec{P} = (2, 0.5, 0.5, 2\times10^6, 0.01)$. At early times, we observe the linear stability regime where $h(q,t) \propto \exp\omega(q)t$, with $\omega = e^2q - \gamma q^2$, where e and γ are proportional to the external strain and film-vapor surface tension, respectively. Defects shorten the period over which this regime can be seen. Their other effect is to renormalize e and γ [25].

For later times, coarsening occurs at the film-vapor interface, leading to a grooved profile as shown in Fig. 2a (with defects $E_c = 10$) and Fig. 2b (without defects $E_c = \infty$) at time $t = 80$, and $m_c = 0.0125$. Parameters are $\vec{P} = (1, 0.775, 0.25, 2\times10^5, 0.1)$. Eventually, the grooves cause the film to break up into islands leav-

ing the substrate partially exposed. Indeed, this is what is observed in the controlled annealing experiments of Ozkan *et al.* [12]. Examination of the b_x field shown in Fig. 2c reveals considerable dislocation activity at the film-substrate interface (thick red line). In particular, dislocations with $b_x > 0$ align themselves at the film-substrate interface to partially screen the film tension. In the island regime, a large dislocation density accumulates at the bottom of each island, exactly as seen in the experiments [12].

A striking feature of these late time configurations is the defect concentration at the bottom of the grooves, as shown in Fig. 2d. These dislocations partially relax the stress concentration and therefore slow growth. To address this in more detail, we carried out extensive numerical simulations of narrow systems with a single groove, $E_c = 1$, and varying m_c. See Fig. 3: top of figure with parameters $\vec{P} = (1, 0.775, 0.25, 2\times10^3, 0.1)$ for $m_c = 0.05$ and times $75 - 100$; bottom of figure with parameters $\vec{P} = (1, 0.9, 0.25, 1\times10^5, 0.04)$ for $m_c = 0.2$ and times $12 - 24$ (little evolution occurs after this time). We initially notched the system and then tracked its growth under stress. The groove attained a well-defined steady-state velocity and shape. Dislocation distributions are clearly evident.

Two main effects are taking place. First, the high concentration of stress at the groove tip causes defects to nucleate and relax some of the stress, if the core energy E_c is not too high. This slows the groove, and blunts its tip. Second, depending on the mobility of the dislocations, the groove tip can "outrun" the defects. Low dislocation mobility leads to a fast tip velocity, where the defects lag behind the tip, while a high mobility gives rise to a slow tip velocity, since the stress-relieving defects can keep pace with the tip. In other words, if the mobility of the dislocations is too low, the film is brittle, while it is ductile for high mobilities. This is clearly illustrated in Fig. 4. For small E_c (where defect nucleation is facilitated), we observe two distinct groove-tip speeds [25] $v_{\min}$ and $v_{\max}$, for $m_c \gg 1$ and $m_c \ll 1$, respectively. Defining a temperature through an Arrhenius form for the mobility $m_c \sim \exp(-E_b/k_B T)$, gives the temperature for a brittle-ductile transition: for $T \gg T_{\text{BDT}} \sim E_b/k_B$, $v_{\text{tip}} \approx v_{\min}$, whereas for $T \ll T_{\text{BDT}}$, $v_{\text{tip}} \approx v_{\max}$. This scenario is analogous to what is observed in materials undergoing fracture: for example, Gumbsch *et al.* [15] studied fracture in tungsten single crystals, and concluded that the brittle-ductile transition required sufficiently mobile dislocations.

To conclude, we have introduced a continuum model of elasticity in a multiphase system, which includes both smooth and singular strains, as well the coupling of those strains to free surfaces. We have applied the general approach to the study of misfitting heteroepitaxial films, and found a brittle to ductile transition, controlled by the dynamics of the interactions between dislocations and free surfaces.

[1] F. C. Frank and J. H. van der Merwe, Proc. R. Soc. London, Ser. A **198**, 205 (1949).

[2] J. W. Matthews and A. E. Blakeslee, J. Cryst. Growth **27**, 118 (1974).

[3] R. J. Asaro and W. A. Tiller, Metall. Trans. **3**, 1789 (1972).

[4] M. Grinfeld, Dokl. Akad. Nauk. SSSR **265**, 836 (1982); Europhys. Lett. **22**, 723 (1993), and references therein.

[5] D. J. Srolovitz, Acta Metall. **37**, 621 (1989).

[6] B. J. Spencer, P. W. Voorhees, and S. H. Davis, Phys. Rev. Lett. **67**, 3696 (1991).

[7] W. H. Yang and D. J. Srolovitz, Phys. Rev. Lett. **71**, 1593 (1993).

[8] J. E. Guyer and P. W. Voorhees, Phys. Rev. Lett. **74**, 4031 (1995).

[9] J. Müller and M. Grant, Phys. Rev. Lett. **82**, 1736 (1999).

[10] K. Kassner and C. Misbah, Europhys. Lett. **46**, 217 (1999). K. Kassner, C. Misbah, J. Müller, and J. Kappey and P. Kohlert, Phys. Rev. E **63**, 036117 (2001).

[11] H. Gao and W. D. Nix, Annu. Rev. Mat. Sci. **29**, 173 (1999).

[12] C. S. Ozkan, W. D. Nix, and H. Gao, Appl. Phys. Lett. **70**, 2247 (1997).

[13] L. Dong, J. Schnitker, R. W. Smith, and D. J. Srolovitz, J. Appl. Phys. **83**, 217 (1998).

[14] K. W. Schwarz, J. Appl. Phys. **85**, 108 (1999); J. Appl. Phys. **85**, 120 (1999).

[15] P. Gumbsch, J. Riedle, A. Hartmeier, and H. F. Fischmeister, Science **282**, 1293 (1998).

[16] A. Onuki and H. Nishimori, Phys. Rev. B **43**, 13649 (1991). See also, C. Sagui, A. M. Somoza, and R. C. Desai, Phys. Rev. E **50**, 4865 (1994).

[17] Generalizing the approach of R. Kobayashi [Physica (Amsterdam) **63D**, 410 (1993)], the Φ's enforce convenient thermodynamics for the vapor, film, and substrate equilibrium phases ($\phi_{\text{eq}} = 0$, 1, or 2, respectively). Namely, we require $\Phi'(\phi_{\text{eq}}) = 0$, where the prime denotes a derivative, and $\Phi(\phi_{\text{eq}}) = \phi_{\text{eq}}$, for $\phi_{\text{eq}} = 0$ or 1, while for $\phi_{\text{eq}} = 2$, $\Phi_{\text{misfit}} = 0$ and $\Phi_{\text{solid}} = 1$. These are satisfied by the choices $\Phi_{\text{misfit}} = -\frac{1}{11}\left(2\phi^6 - 12\phi^5 + 15\phi^4 + 20\phi^3 - 36\phi^2\right)$, and $\Phi_{\text{solid}} = -\frac{3}{132}\left(19\phi^6 - 81\phi^5 + 60\phi^4 + 135\phi^3 - 177\phi^2\right)$.

[18] L. Landau and E. M. Lifshitz, *Theory of Elasticity* 2nd ed. (Pergamon Press, Oxford 1986).

[19] F. R. N. Nabarro, *Theory of crystal dislocations* (Dover Publications, New York 1967).

[20] D. R. Nelson and B. I. Halperin, Phys. Rev. B **19**, 2457 (1979).

[21] The extension to three dimensions is straightforward, but requires a tensorial χ.

[22] M. Haataja, unpublished. M. Haataja, J. Müller, A. D. Rutenberg, and M. Grant, unpublished.

[23] The Airy stress function χ is found in the different phases by solving $\nabla^4 \chi + \frac{1}{\ell^4}(1 - \Phi_{\text{solid}})\chi = \frac{Y}{4}\Phi_{\text{solid}}\epsilon_{ij}\nabla_i b_j$, which incorporates the necessary boundary conditions, where Y denotes the Young's modulus, and ℓ is a small length of order the interface thickness (our results correspond to $\ell/R \ll 1$, where R is a macroscopic length, and are independent of ℓ). This ensures, for example, that the defects have only short-range interactions $\sim \ell$ in the vapor phase, and that they interact via the Peach-Koehler force in the solid phases. The inhomogeneous term gives rise to a thickness-dependent dislocation self-energy [19], which is an essential ingredient [2,22]. Also, note that the back-coupling variable $\beta(\vec{r}) \equiv \epsilon_{ij}\delta F/\delta(\nabla_i b_j)$ satisfies $\nabla^4 \beta(\vec{r}) + \frac{1}{\ell^4}(1 - 4\Phi_{\text{solid}}(\vec{r}))\beta(\vec{r}) = \frac{\delta_{ij}}{4\kappa}\nabla^2\sigma_{ij}(\vec{r}) + \frac{1}{8\mu}[\varepsilon_{ik}\varepsilon_{jl}\nabla_k\nabla_l\sigma_{ij}(\vec{r}) - \frac{\delta_{ij}}{2}\nabla^2\sigma_{ij}(\vec{r})]$.

[24] The smooth strains give rise to long-range forces via $m \equiv \int_{\vec{r}',\vec{r}''} G(\vec{r},\vec{r}')\nabla_i'\nabla_j'[\Phi_{\text{solid}}(\vec{r}')M_{ij}(\vec{r}',\vec{r}'')\Phi_{\text{misfit}}(\vec{r}'')]$, and, $n \equiv [\Phi_{\text{misfit}}(\vec{r})\delta_{ij}/2 - \nabla_i\nabla_j\int_{\vec{r}'} G(\vec{r},\vec{r}')\Phi_{\text{misfit}}(\vec{r}')]^2$, where $\nabla^2 G(\vec{r},\vec{r}') = \delta(\vec{r} - \vec{r}')$ and $M_{ij}(\vec{r}',\vec{r}'') = \nabla_i\nabla_j G(\vec{r}',\vec{r}'') - \delta(\vec{r}' - \vec{r}'')\delta_{ij}/2$,

[25] Of course, if the dislocations are sufficiently mobile no buckling instability takes place [2]

FIG. 1. Scaled amplitude of growth modes ω^* as a function of scaled wave number q^* in the early-time linearly unstable regime. Diamonds $E_c = 1$, squares $E_c = 50$, circles $E_c = \infty$ (no defects), dashed line is linear stability theory. Data scaled by maximum growth rate and wavenumber for restabilization, both of which increase with increasing E_c. Inset shows configurations for $E_c = 1, 50, \infty$, from top to bottom. Four times are shown for each; grooves deepen with time for all.

FIG. 2. (a) Configuration with defects (green is film, orange is substrate, blue is vapor). (b) Without defects (note faster groove growth). (c) Density of defects (b_x) from (a). Note pile up at film-substrate interface and in high curvature regions. (d) Magnification of part of (c) showing $\vec{b}$.

FIG. 3. (a) Sequence of groove tips in *brittle* region, outrunning dislocations, which are shown as Burger's vectors. (b) Sequence of groove tips in *ductile* region, where dislocations keep pace with tip.

FIG. 4. Tip speed vs. natural log of climb mobility for various E_c as indicated. Note well defined transition from brittle region to ductile region with increasing mobility.
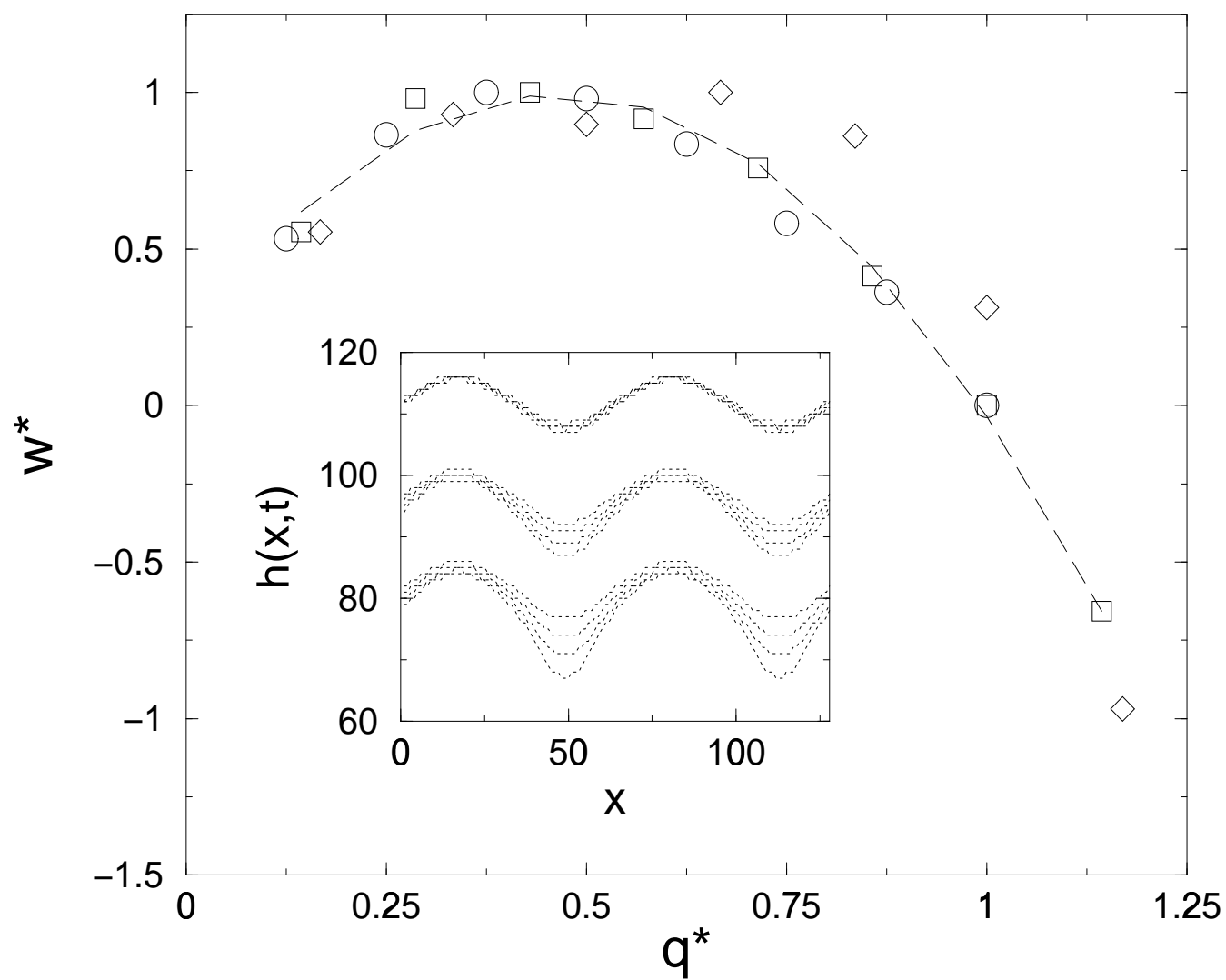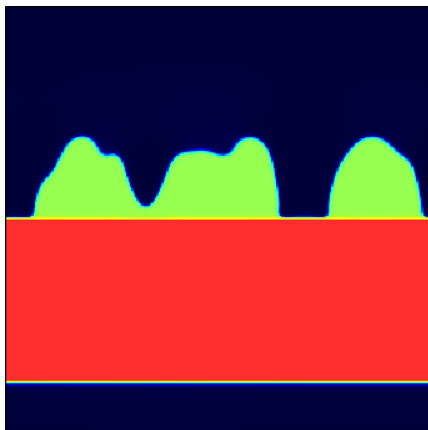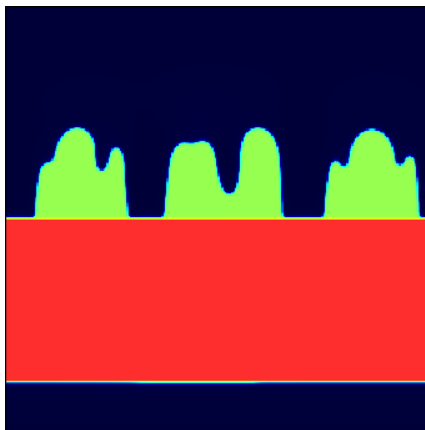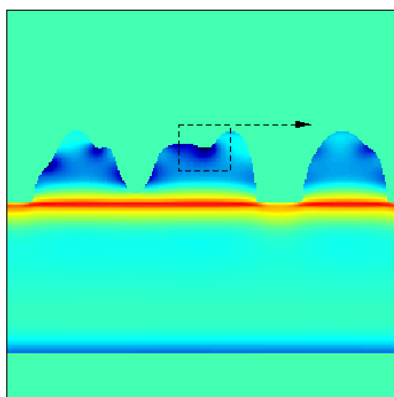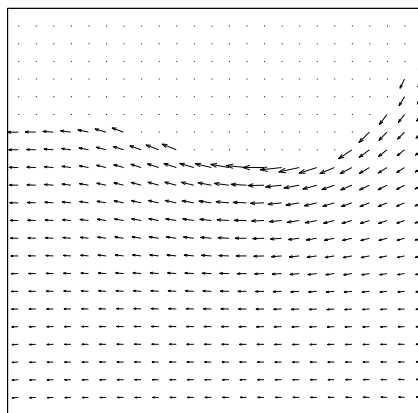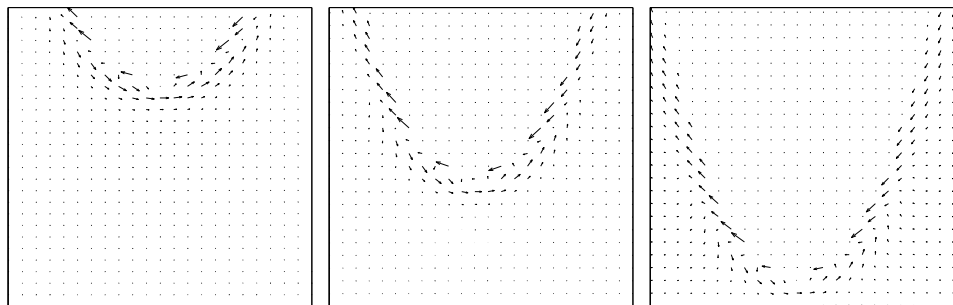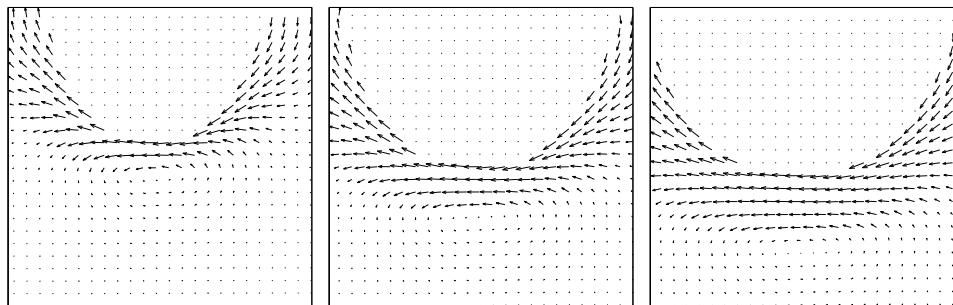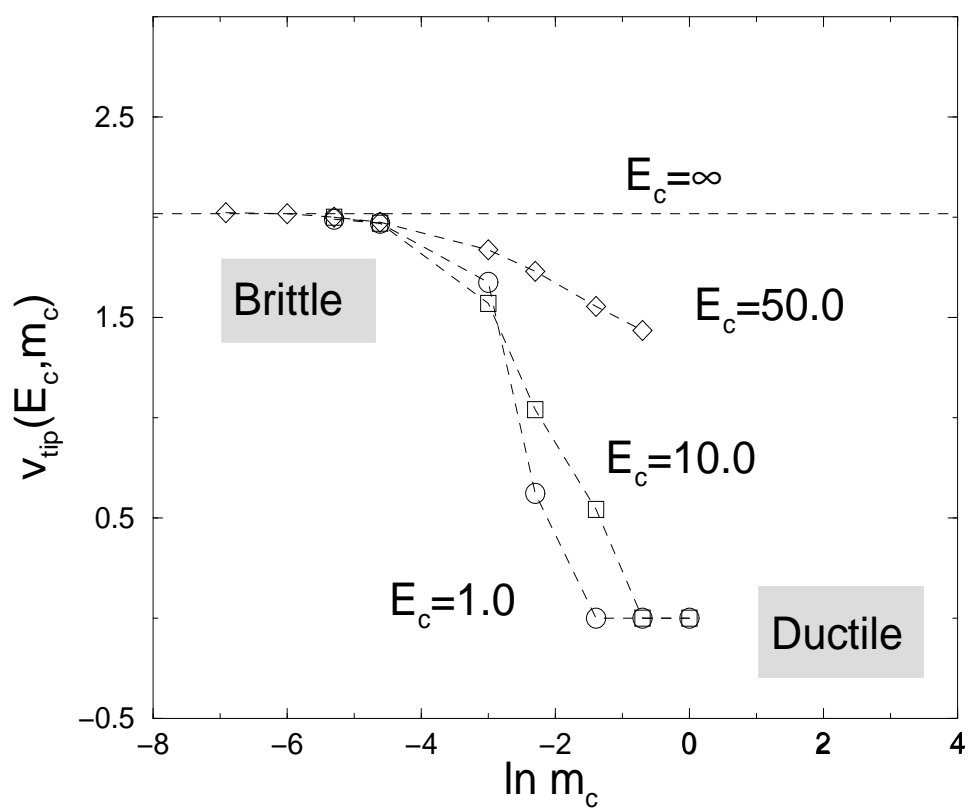
4

Figure 1.

(a)

(b)

(c)

(d)

Figure 2.

(a)

(b)

Figure 3.

Figure 4.